

## DISSIPATION IN COMPRESSIBLE MHD TURBULENCE

JAMES M. STONE, EVE C. OSTRIKER

Department of Astronomy, University of Maryland, College Park, MD 20742-2421

AND

CHARLES F. GAMMIE

Center for Astrophysics, MS-51, 60 Garden St., Cambridge MA 02138

*Draft version October 16, 2018*

### ABSTRACT

We report results of a three dimensional, high resolution (up to  $512^3$ ) numerical investigation of supersonic compressible magnetohydrodynamic turbulence. We consider both forced and decaying turbulence. The model parameters are appropriate to conditions found in Galactic molecular clouds. We find that the dissipation time of turbulence is of order the flow crossing time or smaller, even in the presence of strong magnetic fields. About half the dissipation occurs in shocks. Weak magnetic fields are amplified and tangled by the turbulence, while strong fields remain well ordered.

*Subject headings:* MHD – turbulence – waves – ISM: kinematics and dynamics – ISM: magnetic fields

### 1. INTRODUCTION

The large linewidths of molecular species in molecular clouds in our Galaxy imply the velocity dispersion  $\sigma_v$  of the gas is much larger than the sound speed  $c_s$  ( $\sigma_v \sim 1 - 10 \text{ km s}^{-1}$ , whereas  $c_s \sim 0.2 - 0.3 \text{ km s}^{-1}$ ; e.g. Solomon et al (1987), Heyer & Schloerb (1997)). Although magnetic field strengths are difficult to measure, the best estimates in such clouds give Alfvén speeds  $v_A$  that are much larger than the sound speed but of order, or somewhat exceeding, the velocity dispersion (e.g. Myers & Goodman (1988), Crutcher et al (1993), Goodman & Heiles (1994), Crutcher (1998)). The dynamics of this gas is of considerable astrophysical interest, as it may govern the rate and character of star formation in our galaxy.

Two notions about the dynamics of molecular clouds have been particularly influential since the first CO maps were made in the 1970s: (1) The turbulent motions in molecular clouds are thought to act as a “turbulent pressure” to support a cloud against self-gravity (cf. Chandrasekhar (1951)). This is motivated by the discrepancy between estimated cloud collapse times  $\lesssim 3 \times 10^6 \text{ yr}$ , after which it is presumed that most of the cloud would turn into stars (violating limits on the Galactic star formation rate), and estimated cloud lifetimes  $\gtrsim 3 \times 10^7 \text{ yr}$ . (2) Supersonic, sub-Alfvénic turbulence is thought to persist for more than a cloud flow crossing time over cloud size  $L$ ,  $t_f(L) = L/\sigma_v = 10^7 \text{ yr} \times (L/10 \text{ pc})(\sigma_v/1 \text{ km s}^{-1})^{-1}$ , because magnetic fields provide a cushion that reduces dissipation rates. In particular Arons & Max (1975) proposed that molecular cloud turbulence may be primarily in Alfvénic motions because for linear-amplitude waves no compressions are involved. Recently, both of these ideas have been called into question. This Letter describes high resolution, three dimensional numerical experiments designed to test the latter idea, with possible implications for the former.

We evaluate the dissipation rate of supersonic, sub-Alfvénic turbulence in the context of an idealized numerical model. Our model is three-dimensional, compress-

ible, ideal (no explicit resistivity, viscosity, or ambipolar diffusion), non-self-gravitating (future papers will discuss the effects of gravity), isothermal (a fair approximation for most of the material in molecular clouds) and has a uniform mass to flux ratio. It is also homogeneous and isotropic, insofar as it considers the evolution of turbulence in a periodic box, where there are no boundaries.

This work builds on earlier results from our group and from others. Gammie & Ostriker (1996; hereafter GO) considered similar issues in a 1 2/3 dimensional model, while Ostriker, Gammie, & Stone (1998; hereafter OGS) considered a 2 1/2 dimensional model. Among other results, GO found that purely Alfvénic turbulence quickly couples to other, compressive waves (see §4 below), and OGS found that independent of initial turbulence levels, magnetically supercritical clouds collapse gravitationally in 5-10 Myr, in the absence of stirring. Padoan & Nordlund (1997) studied the evolution of Mach 5 decaying MHD turbulence in 3D cloud models with  $\beta = 2$  and 0.02, and MacLow et al (1998) studied the evolution of Mach 5 decaying MHD turbulence for  $\beta = 1$  and 0.04; both groups concluded the dissipation time in such models is short. This work differs from these last two in that we consider *driven* turbulence and turbulence decaying from *saturated* initial conditions, thus avoiding transients associated with a particular choice of initial conditions.

### 2. METHOD AND PARAMETERS

We integrate the equations of compressible, ideal MHD using the ZEUS code (Stone & Norman 1992a; 1992b). The model is a cubic, periodic box of size  $L$  containing a plasma of uniform density  $\rho_0$  threaded by an initially uniform magnetic field  $\mathbf{B}_0 = (B_0, 0, 0)$ . The sound speed  $c_s$  is constant in both space and time. Grid resolutions vary between  $32^3$  and  $512^3$ . To allow a study of turbulent mixing, all models evolve a passive contaminant which initially fills a cylindrical volume in the center of the grid oriented with the symmetry axis parallel to  $\mathbf{B}_0$  and with diameter and axial length equal to  $L/2$ .

We drive turbulence by adding velocity perturbations  $\delta\mathbf{v}$  at time intervals  $\Delta t$  with  $\Delta t L/c_s = 0.001$ . Each  $\delta\mathbf{v}$  is an independent realization of a Gaussian random field with power spectrum  $|\delta\mathbf{v}_k|^2 \propto k^6 \exp(-8k/k_{pk})$  (we choose  $k_{pk} = 8 \times (2\pi/L)$ ), subject to the constraint that  $\nabla \cdot \delta\mathbf{v} = 0$ . Since the input perturbations are incompressible, this is a minimally dissipative way of stirring the model. The perturbations are normalized so that the kinetic energy input rate  $\dot{E} = \text{const.}$ , and no net momentum is added to the box,  $\int \rho \delta\mathbf{v} = 0$ .

In addition to  $\Delta t L/c_s$  and  $k_{pk} L/2\pi$ , two dimensionless parameters characterize our models:  $\beta$  and  $\dot{E}$ . We study values of  $\beta = 0.01$  (strong field), 0.1 (moderate field), 1.0 (weak field), and  $\infty$  (pure hydrodynamics). Corresponding physical values of the magnetic field are given by  $B = 1.4\mu\text{G} \beta^{-1/2} (T/10\text{ K})^{1/2} (n_{H_2}/10^2\text{ cm}^{-3})^{1/2}$ . In this Letter we present only models with  $\dot{E}/\rho_0 L^2 c_s^3 = 10^3$ , but comment on results drawn from other models.

To transform dimensionless parameters to astronomically relevant quantities, one may independently choose values for  $\rho_0$ ,  $c_s$ , and  $L$ . As an example, consider a cloud clump of size  $L = 2$  pc, mean density  $n_{H_2} = 10^3\text{ cm}^{-3}$ , and temperature  $T = 10$  K. Then the sound speed is  $c_s \approx 0.2\text{ km s}^{-1}$ . This implies the sound crossing time  $t_s \equiv L/c_s \sim 10$  Myr, and driving power  $\dot{E} = 0.4L_\odot$ . For  $\beta = 0.01$  the magnetic field strength is  $B = 44\ \mu\text{G}$  and the Alfvén speed is  $v_A \approx 2\text{ km s}^{-1}$  with the corresponding Alfvén wave crossing time  $t_A \equiv L/v_A \sim 1$  Myr. For the moderate (weak) field case the field strength is reduced to  $14\mu\text{G}$  ( $4.4\mu\text{G}$ ), so that  $v_A = 0.6(0.2)\text{ km s}^{-1}$  and  $t_A = 3(10)$  Myr. A typical velocity dispersion in a cloud with these properties is  $1\text{ km s}^{-1}$ , so  $t_f(L) = 2$  Myr.

### 3. RESULTS

First consider driven turbulence models. Evolution of the total energy in fluctuations  $E \equiv E_K + E_B \equiv \int (\rho v^2/2 + (B^2 - B_0^2)/(8\pi))$  for  $\beta = 1$  models computed at resolutions of  $32^3$  through  $512^3$  shows that in each case,  $E$  rises steeply and then reaches a final, saturated value. The amplitude of  $E/\rho L^3 c_s^2$  depends quite sensitively on the numerical resolution; grids of  $32^3$ ,  $64^3$ ,  $128^3$ ,  $256^3$  and  $512^3$  zones give saturated energy levels of 9.4, 13, 16, 17, and 18 respectively. Note there is a clear (although slow) trend towards convergence in these numbers, although since we have not used identical realizations of the forcing spectrum in each case we cannot measure the rate of convergence precisely. In the saturated state the dissipation rate balances the input power  $\dot{E}$ , and one may define the dissipation timescales  $t_{diss} \equiv E/\dot{E}$  and  $t_{diss}^K \equiv E_K/\dot{E}$ ; these may be compared to the flow crossing time at the scale  $\lambda_{pk} = L/8$  at which the turbulence is driven,  $t_f(\lambda_{pk}) \equiv \lambda_{pk}/\sqrt{2E_K}$  (which we hereafter abbreviate as  $t_f$ ).<sup>1</sup> All the models saturate at times  $\sim t_f$ . For the  $\beta = 1$  model at  $512^3$  resolution, we find  $t_{diss}/t_f = 0.75$  and  $t_{diss}^K/t_f = 0.54$ .

Where does the energy go in the numerical models? One route to dissipation is via shocks. ZEUS uses an artificial viscosity to capture shocks, and so the shock dissipation

rate can be measured by integrating the work done by artificial viscosity over space and time. This accounts for about 50% of the dissipation. Another route is through a turbulent cascade like that which occurs in incompressible hydrodynamic (e.g. Landau & Lifshitz (1987)) and MHD (e.g. Goldreich & Sridhar (1995)) turbulence; there non-linear interactions transfer energy to progressively smaller and smaller scales until a dissipation scale is reached and the energy is thermalized. Since the present models include no explicit resistivity, viscosity, or ambipolar diffusion to thermalize the energy at small scales, energy is finally lost through numerical effects at the grid scale.<sup>2</sup> A completely satisfactory study would include astrophysically appropriate values for the microscopic diffusion coefficients and close the energy equation, but we have not done so here because the task is prohibitively expensive. This is one of the major challenges for future work.

How does the dissipation rate vary with magnetic field strength? Figure 1a shows the evolution of  $E$  for various  $\beta$  at a resolution of  $256^3$ . The amplitude of  $E$  increases monotonically with field strength (decreasing  $\beta$ ); hence dissipation decreases as field strength increases. In Table 1, we give the values for the energy in the saturated state (averaged over time  $t = 0.2 - 0.3t_s$ ), as well as the saturated-state dissipation times for the four models displayed. From the values in the Table, the change in  $E$  with  $\beta$  is not large, amounting to only a  $\sim 30\%$  increase in the  $E$  saturation amplitude as  $\beta$  varies from  $\infty$  to 0.01. The dissipation times for saturated turbulence all lie in the range  $\sim 0.5 - 0.8t_f$ , with slightly longer dissipation times for stronger- $B_0$  models.

The structure of driven compressible MHD turbulence changes as the field strength is varied. Figure 2 shows the logarithm of the density along three faces of the computational volume, representative magnetic field lines, and an isosurface of the passive contaminant after saturation for both  $\beta = 0.01$  and  $\beta = 1$  models computed at a resolution of  $256^3$ . In both cases, the density is compressed into small scale knots and filaments; in the  $\beta = 0.01$  model these are elongated in the direction parallel to the field. The mass (volume) weighted mean of  $\log(\rho/\rho_0)$  in the strong magnetic field model is 0.28 (-0.29), whereas for the weak field model it is 0.20 (-0.22), indicating the density contrasts are larger for strong fields at fixed turbulent Mach number. The maximum density in the strong field model is 83; for the weak field model it is 44. The passive contaminant is confined to a narrow range of flux tubes for  $\beta = 0.01$ , indicating that cross-field diffusion is small; for  $\beta = 1$  it diffuses isotropically.

There is a tendency toward equipartition of kinetic and magnetic energy in all the models. From Table 1, the turbulent magnetic energy  $\delta E_B$  is between 30%-60% of  $E_K$ . In the weak field case, significant amplification of the magnetic field is produced by the turbulence, so that after saturation the energy in the fluctuations in the field is ten times larger than that in the mean field. In the weakly magnetized model the field lines are thoroughly tangled (Fig. 2b). In the strong field model the field lines are relatively well ordered (Fig. 2a), as expected (e.g. Weiss

<sup>1</sup> $t_f$  is often referred to as the ‘‘eddy turnover time’’ for incompressible turbulence; for compressible flows the present terminology is preferred.

<sup>2</sup>Explicitly resistive experiments done by us capture another 20% of the dissipation. The relative importance of the different routes to dissipation at small scales will depend on the precise values of the microscopic diffusion coefficients (e.g. Biskamp & Welter (1990))

TABLE 1  
DISSIPATION CHARACTERISTICS OF SATURATED MHD TURBULENCE

model	$\beta$	$E/\rho L^3 c_s^2$	$E_K/\rho L^3 c_s^2$	$\frac{\delta E_B}{E_K}$	$\frac{t_{diss}}{t_f}$ <sup>a</sup>	$\frac{t_{diss}^K}{t_f}$ <sup>a</sup>	$\frac{t_{dec}}{t_f}$ <sup>a</sup>	$\frac{t_{dec}^K}{t_f}$ <sup>a</sup>
A	0.01	20.3	13.0	0.56	0.83	0.54	0.82	0.65
B	0.1	18.9	11.8	0.61	0.74	0.46	0.69	0.39
C	1.0	17.0	12.9	0.32	0.70	0.53	0.58	0.37
D	$\infty$	15.4	15.4	0	0.69	0.69	0.40	0.40

<sup>a</sup> $t_{diss}$ ,  $t_{diss}^K$ ,  $t_f$ ,  $t_{dec}$ , and  $t_{dec}^K$  defined in text

(1966)).

Next consider models of decaying turbulence. The initial conditions are taken from the saturated driven models presented above. Figure 1b shows the evolution of  $E$  for decay from saturated initial conditions for various magnetic field strengths. At late times the decay of  $E$  follows a power law in time, with index between 0.8-0.9 (consistent with the finding of MacLow et al (1998)). This implies that the dissipation time varies with time. We define decay times  $t_{dec}$  ( $t_{dec}^K$ ) as the time taken for 50% of the *initial* energy (kinetic energy) to be lost; values for the decay time in these decay runs are given in Table 1. For all models, the decay times are in the range 0.4-0.8  $t_f$ , comparable to the range of steady-state dissipation times.

The decay rate measured here could in principle differ substantially from decay simulations that begin with unsaturated initial conditions. To investigate this possibility, we have computed the decay of supersonic turbulence from initial conditions in which the magnetic and velocity field perturbations are taken from the saturated, driven model A, but the density is reset to a uniform value. The result is plotted as a dashed line in Figure 1b. The corresponding decay times are  $t_{dec}/t_f = 0.80$  and  $t_{dec}^K/t_f = 0.68$ , nearly identical to those for Model A's decay.

Finally, to make contact with other studies of decaying MHD turbulence, we have performed simulations which begin with a uniform density and magnetic field, and velocity perturbations that follow a  $k^{-2}$  spectrum normalized to have the same initial energy as our driven turbulence simulations at saturation. The result is shown as a dotted line in Figure 1b; the decay times for this model are  $t_{dec}/t_f = 1.0$  and  $t_{dec}^K/t_f = 0.6$ , again comparable to the other dissipation times we have found. Thus we conclude that turbulent decay times are not strongly affected by specifics of initial conditions. The energy decay times found for 2.5D models (OGS) are a factor 1.5-1.75 times larger than those obtained here with 3D models.

#### 4. DISCUSSION

Taking together the results of all the models presented here, our conclusion is that compressible MHD turbulence dissipates rapidly – in less than one flow crossing time at the energy-containing scale – regardless of the field strength, and of the details of the initial or ongoing energy input characteristics. For our model 2 pc cloud, the turbulent dissipation time is always less than 1/4 Myr when

the turbulent scale is 1/8 the size of the cloud, and less than 2 Myr when the largest turbulence scale is the same size as the cloud. For GMCs, with flow crossing times  $\sim 5-10$  Myr and the largest energy-containing scale probably comparable to the cloud scale, our results imply that without continual energy input, the observed nonthermal linewidths would decay in less than the cloud lifetimes. The energy input rate required to keep the turbulence going is not large, however, amounting to only 0.4  $L_\odot$  in mechanical power, input at a scale 0.25 pc, for the parameters of our model cloud.

Why are magnetic fields unable to reduce dissipation in supersonic, sub-Alfvénic turbulence? One might have expected that nonlinear but still incompressive Alfvén waves could safely store a significant fraction of the energy. But for the nonlinear amplitudes  $\delta v_A \gtrsim 0.1 v_A$  and  $\beta \equiv c_s^2/v_A^2 < 1$  conditions which are likely to obtain in molecular clouds, couplings between the MHD wave families are strong. Even a circularly polarized Alfvén wave, which is an exact nonlinear solution to the equations of motion, is dynamically unstable to decay into compressive motions (Sagdeev & Galeev (1969), Goldstein (1978)). Thus a spectrum of Alfvén waves of nonlinear amplitude can be quickly converted to compressive motions, which decay rapidly.

The dissipation of turbulent energy may be an important heat source within molecular clouds. From our driven-turbulence models, where energy is input at 1/8 the size of the cloud, we find that the volume dissipation rate of energy is  $\dot{E}/L^3 = 7.5\rho_0\sigma_v^3/L$ ; for clouds where the energy is primarily contained on the largest scale possible, the dissipation rate might be reduced by a factor 8 (for a given velocity dispersion). The corresponding volume-averaged heating rate is  $\Gamma_{turb} = 5.8 \times 10^{-27} (n_H/1 \text{ cm}^{-3}) (\sigma_v/\text{km s}^{-1})^3 (L/\text{pc})^{-1} \text{ erg cm}^{-3} \text{ s}^{-1}$  for the smaller-scale turbulence case, with a factor 8 reduction possible. Except for conditions where the velocity dispersion approaches the sound speed (e.g. dense cores of size  $\sim 0.1$  pc, cf. Goodman et al 1998), this *average* turbulent heating rate exceeds the cosmic-ray heating rate, and in large clouds where the velocity dispersion is large,  $\Gamma_{turb}$  may compete with photoelectric heating (e.g. Spitzer (1978)). Locally, however, turbulent dissipation may greatly exceed other sources of heating; future studies will characterize the localization of turbulent heating.

## REFERENCES

- Arons, J. & Max, C. E. 1975, ApJ, 196, L77  
 Biskamp, D., & Welter, H. 1990, Phys. Fl. B 2, 1787  
 Chandrasekhar, S. 1951, Proc. Roy. Soc A210, 26  
 Crutcher, R. M., Troland, T. H., Goodman, A. A., Heiles, C., Kazes, I., & Myers, P. C., ApJ, 407, 175  
 Crutcher, R. M. 1998, in Interstellar Turbulence, Proceedings of the 2nd Guillermo Haro Conference, Eds. Franco, J. & Carraminana, A., Cambridge University Press  
 Gammie, C. F. & Ostriker, E. C. 1996, ApJ, 466, 814 (GO)  
 Goldreich, P. & Sridhar, S. 1995, ApJ, 438, 763  
 Goldstein, M.L. 1978, ApJ, 219, 700  
 Goodman, A. A., & Heiles, C. 1994, ApJ, 424, 208  
 Goodman, A.A., Barranco, J.A., Wilner, D.J., and Heyer, M.H. 1998, ApJ, in press  
 Heyer, M. H., Schloerb, F. P. 1997, ApJ, 475, 173  
 Landau, L.D., & Lifshitz, E.M. 1987, Fluid Mechanics (New York: Pergamon Press)  
 MacLow, M. M., Klessen, R. S., Burkert, A., Smith, M. D., & Kessel, O. 1998, preprint  
 Myers, P. C., & Goodman, A. A. 1988, ApJ, 326, L27  
 Myers, P. C., & Goodman, A. A. 1991, ApJ, 373, 509  
 in Star Formation Near and Far, Eds. S. Holt & L. Mundy, Woodbury NY: AIP Press, p. 51  
 Ostriker, E.C., Gammie, C.F., & Stone, J.M. 1998, ApJ, submitted (OGS)  
 Padoan, P., & Nordlund, A. 1997, preprint  
 Sagdeev, R. Z., & Galeev, A. A. 1969, Nonlinear Plasma Theory (New York: W. A. Benjamin)  
 Stone, J. M., in "Interstellar Turbulence," eds. J. Franco & A. Carraminana (Cambridge U. Press)  
 Solomon, P. M., Rivolo, A. R., Barrett, J., & Yahil, A. 1987, ApJ, 319, 730  
 Spitzer, L. 1978, Physical Processes in the Interstellar Medium (Wiley: NY)  
 Stone, J. M. & Norman, M. L. 1992a, ApJSupp, 80, 753  
 Stone, J. M. & Norman, M. L. 1992b, ApJSupp, 80, 791  
 Weiss, N.O. 1966, Proc. Roy. Soc. A 293, 310

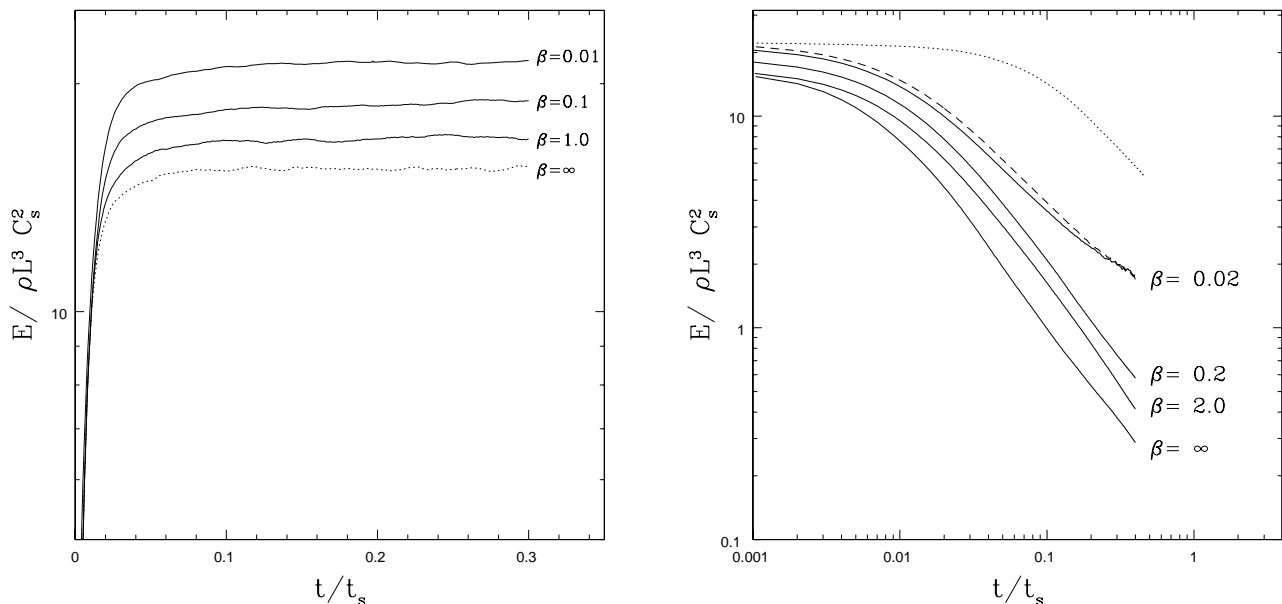
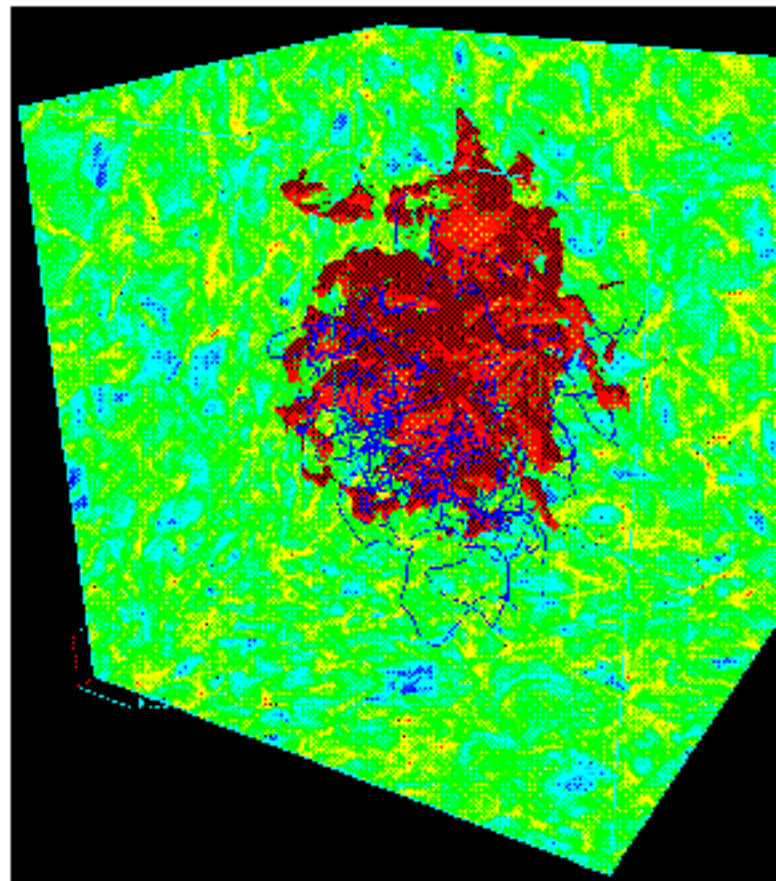
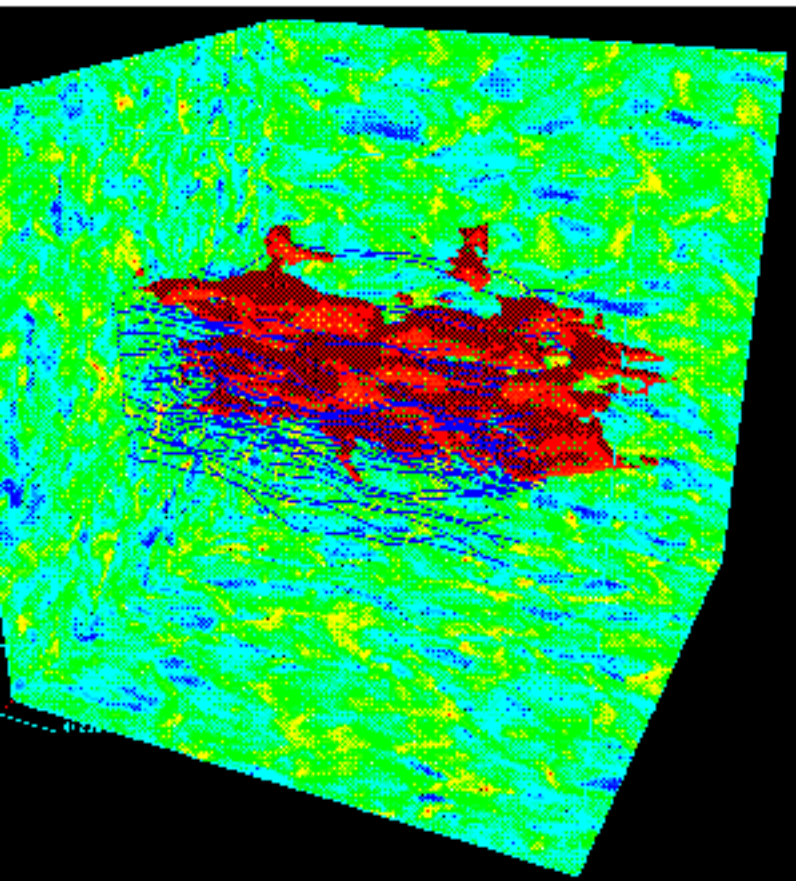


Fig. 1.— Total energy in fluctuations  $E$  versus time for various  $\beta$  at a numerical resolution of  $256^3$  *Left*: forced models *Right*: decaying models. Solid curves – decay from saturated state; dashed curve – decay of density-reset saturated state; dotted line – decay of  $k^{-2}$  velocity spectrum

Fig. 2.— Images of the logarithm of the density (colors) on three faces of the computational volume, representative magnetic field lines (dark blue lines), and isosurface of the passive contaminant (red) after saturation. *Left:*  $\beta = 0.01$   
*Right:*  $\beta = 1$



— Images of the logarithm of the density (colors) on three faces of the computational volume, representing the field lines (dark blue lines), and isosurface of the passive contaminant (red) after saturation. *Left*  $\tau = 1$